Optimization and benchmarking of a perturbative Metropolis Monte Carlo quantum mechanics/molecular mechanics program

Jonas Feldt, Sebastião Miranda, Frederico Pratas, Nuno Roma, Pedro Tomás, and Ricardo A. Mata

Citation: The Journal of Chemical Physics **147**, 244105 (2017);
View online: https://doi.org/10.1063/1.5009820
View Table of Contents: http://aip.scitation.org/toc/jcp/147/24
Published by the American Institute of Physics

Optimization and benchmarking of a perturbative Metropolis Monte Carlo quantum mechanics/molecular mechanics program

Jonas Feldt,[1] Sebastião Miranda,[2] Frederico Pratas,[2] Nuno Roma,[2] Pedro Tomás,[2] and Ricardo A. Mata[1]
[1]*Institut für Physikalische Chemie, Universität Göttingen, Tammannstrasse 6, D-37077 Göttingen, Germany*
[2]*INESC-ID/IST, Universidade de Lisboa, Rua Alves Redol, 1000-029 Lisboa, Portugal*

(Received 20 October 2017; accepted 1 December 2017; published online 22 December 2017)

In this work, we present an optimized perturbative quantum mechanics/molecular mechanics (QM/MM) method for use in Metropolis Monte Carlo simulations. The model adopted is particularly tailored for the simulation of molecular systems in solution but can be readily extended to other applications, such as catalysis in enzymatic environments. The electrostatic coupling between the QM and MM systems is simplified by applying perturbation theory to estimate the energy changes caused by a movement in the MM system. This approximation, together with the effective use of GPU acceleration, leads to a negligible added computational cost for the sampling of the environment. Benchmark calculations are carried out to evaluate the impact of the approximations applied and the overall computational performance. *Published by AIP Publishing.* https://doi.org/10.1063/1.5009820

I. INTRODUCTION

The theoretical treatment of chemical systems in solution is still a major challenge today. Although much progress has been made in the description of condensed phase through parametrised molecular mechanics (MM) force fields,[1–3] we are still far from a well-defined standard approach to reactivity in solution. Whenever an explicit description of the electronic structure is required, one is left with the question of how to include the solvent effects in the quantum mechanical (QM) calculations. The use of hybrid QM/MM models for condensed phase has been a popular approach for several years. Through the use of multiscale modeling, the application range of QM has been expanded to fields such as enzymatic catalysis[4–6] and surface and material sciences,[7–9] just to name a few. However, this all comes at a cost. Even a rather simple QM calculation on a dozen atoms can outweigh the cost of MM energy and gradient evaluations in a complete simulation box.

Particularly limiting to the application of QM/MM methods is the problem of configurational sampling, perhaps even more than the limitation in the QM system size. In order to sample the configurational space of interest, simulations spanning over hundreds of picoseconds (or even nanoseconds) may be required. These are, however, prohibitively expensive. In the case of molecular dynamics (MD), all components of the system have to evolve concurrently. This requires several thousand QM calculations. This is mainly due to the environment and its large number of degrees of freedom. Even when the impact on the computed property is small, proper configurational sampling is required, otherwise one will be at risk of introducing a bias.

Sequential QM/MM approaches are oftentimes used in this context. Classical simulations can generate the ensemble followed by a limited number of QM/MM calculations on a subset of configurations. A recent study[10] investigated systematically the impact of the force field used in the classical simulations on the final QM/MM results. It turns out that the accuracy is mostly determined by the latter choice and that standard transferable force fields can lead to very large errors. Except for a tedious system-specific reparametrization, only a sampling at the QM/MM level can avoid this error completely.

Continuum solvation models are a different approach to describe solvation which altogether avoid the sampling problem. The most popular examples include the conductor-like screening model (COSMO),[11] the polarizable continuum model (PCM),[12] or the somewhat more recent solvation model based on the solute density (SMD).[13] This class of methods describe the solvent as a continuum around the solute. Common to all of them is the construction of a cavity on which surface charges are computed to describe the electrostatic interaction. The cavity can, for example, be constructed of scaled van der Waals (vdW) radii or as the solvent accessible surface. The results are rather sensitive to the construction of the cavity. The surface charges are determined self-consistently and therefore allow for mutual polarization between the solute and the continuum.

The COSMO-RS[14] model improves upon this continuum description. The approximate structure of the solvent is taken into account by computing the probability distribution of the screening charge density from a COSMO calculation. Surface patches are constructed and the electrostatic interaction is computed as a sum of pairwise interactions of these patches. The perfectly adapted charges of the continuum are therefore substituted by the more realistic surface patches. Additional terms for the description of hydrogen bonds and dispersion effects are added. Also models like PCM or SMD add further terms, e.g., for the formation of the cavity and the dispersion interaction.[12,13] These terms are commonly related to macroscopic properties like the surface tension.

Continuum models are an effective way to include the polarization of the solvent molecules which in a simple QM/MM approach is often neglected. However, the description of the entropic effect is not very well defined due to the lack of solvent degrees of freedom. Also specific and directional interactions like hydrogen bonds are not included or only described in an approximate way. Heterogeneous environments like solvent mixtures, ions in solution, or even protein environments can be difficult to describe with continuum models.

A very different approach is the reference interaction site model[15,16] (RISM) which instead of exploring the phase space is based on spatial distributions. By solving an Ornstein-Zernike type integral equation, the solvation structure is obtained and analytical expressions for the solvation thermodynamics can be derived. In order to solve these equations, an additional closure relation is required, e.g., the hypernetted chain (HNC) closure[17,18] or the Kovalenko-Hirata (KH) closure.[19] This approach is computationally very efficient since no explicit simulation is required. A recent development by Kast and co-workers computes the expensive electrostatic interactions in reciprocal space reducing the computational costs even further.[20]

However, RISM can also lead to thermodynamic inconsistent results. For example, the pressure can be calculated directly and indirectly from the compressibility or internal energy and these three results can differ greatly. Furthermore, interaction sites of molecular species are considered non-bonded by the widely used HNC closure relation which results, for example, in a non-physical dependence on the so-called auxiliary sites that just label a fixed point inside of the molecule. The excess chemical potential is overestimated for hydrophobic hydration, and steric constraints are violated.[21] In fact, the choice of the right closure relation is not clear as other relations have different problems, like the KH closure relation which is known to create too broad distributions.[22]

Perturbative Monte Carlo QM/MM (PMC QM/MM), first suggested by Truong and Stefanovitch,[23] was a promising alternative to solve the sampling problems in QM/MM calculations. In this method, the coupling between the two regions is approximated by first-order perturbation theory, leading to a simple electrostatic 2-body term. This allows for the effective application of Metropolis Monte Carlo, even though no efficient implementation has been presented to date. There is also little information on how the method fairs in a realistic simulation case, involving hundreds of solvent molecules and with extended simulation times. The algorithm has to be designed to take full advantage of the separation between the QM and MM calculations. This was not possible at the time the method was proposed, given that hybrid architectures were not available. In this work, we discuss a multi-device parallel approach to PMC, using the Metropolis MC sampling and a mixed QM/MM method for the energy calculation.

In Sec. II, we start by reviewing the original method and discuss its extension to periodic systems. Given that examples in the application of PMC are somewhat limited, we compare the results of a standard PMC implementation to full QM/MM results. We then proceed to analyse the impact of specific approximations used in our scheme, in particular the update of the QM system density and the numerical integration grid. We also briefly discuss the GPU acceleration although the interested reader should refer to Ref. 24 for more information. A series of benchmark applications are discussed, comparing with experiment and previous condensed phase calculations.

II. METHOD

Simulation systems in a QM/MM run are composed of a region of interest (in some cases referred to as active site) and an immersive environment. The latter can be a protein and/or solvent molecules. For simplicity, we will mostly refer to solvent environments in this work. Figure 1 shows a schematic example of how such a system could look like. We reduce it to a very simple case: a single molecule, which is treated at the QM level, and two solvent molecules, treated at the MM level. By applying Metropolis MC, a molecule will be randomly picked and then translated and rotated to generate a new structure. This last MC step will be either accepted or rejected, according to the resulting energy change.

The total energy in a QM/MM calculation can be expressed as

$$E_{\mathrm{QM/MM}} = E_{\mathrm{QM}} + E_{\mathrm{MM}} + E^{\mathrm{C}}_{\mathrm{QM/MM}} + E^{\mathrm{vdW}}_{\mathrm{QM/MM}}, \qquad (1)$$

where the first two terms on the right-hand side represent the internal energy of the QM and MM subsystems, and the last the interaction between the two, Coulomb ($E^{\mathrm{C}}_{\mathrm{QM/MM}}$) and van der Waals (vdW, $E^{\mathrm{vdW}}_{\mathrm{QM/MM}}$).

If a molecule in the MM subsystem is moved, all terms in Eq. (1) will be affected, not only the force field terms. Charges are being moved and the wave function/density of the QM subsystem will change as a result of this variation. This would require a new SCF cycle for each MC step. Since the computational efficiency of the Monte Carlo method relies on the use of 2-body potentials, there really is no advantage in the use of conventional QM/MM in this context.

Truong and Stefanovich[23] proposed the use of first order perturbation theory to approximate the electrostatic coupling between the QM and MM subsystems. If a set of partial charges is moved from the position vector set $\{\mathbf{r}_\alpha\}$ to a new $\{\mathbf{r'}_\alpha\}$, the energy change in the terms E_{QM} and $E^{\mathrm{C}}_{\mathrm{QM/MM}}$ will be given by

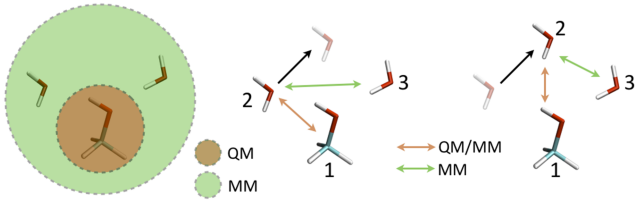

FIG. 1. A system composed of one QM molecule (1, red) and two MM solvent molecules (2 and 3, green). For each MC step, the difference in energy between the molecule moved (2) and every other molecule has to be computed, but at different levels of theory.

$$\Delta(E_{\mathrm{QM}} + E^{\mathrm{C}}_{\mathrm{QM/MM}}) = \langle \Psi' | \hat{H}^{\mathrm{QM}} + \sum_i \sum_\alpha \frac{q_\alpha}{|\mathbf{r}'_\alpha - \mathbf{r}_i|} | \Psi' \rangle - \langle \Psi | \hat{H}^{\mathrm{QM}} + \sum_i \sum_\alpha \frac{q_\alpha}{|\mathbf{r}_\alpha - \mathbf{r}_i|} | \Psi \rangle + \sum_A \sum_\alpha{}' \left(\frac{q_\alpha Z_A}{|\mathbf{r}'_\alpha - \mathbf{r}_A|} - \frac{q_\alpha Z_A}{|\mathbf{r}_\alpha - \mathbf{r}_A|} \right). \tag{2}$$

The indices i and A run over the solute electrons and nuclei, respectively. The wave function Ψ is calculated for the initial position of the lattice, with the wave function Ψ' being the converged solution for the new charge position. Partial sums restricted to the charges which have been moved are marked with a prime. As it can be observed, this amounts to a full new calculation of the QM subsystem energy although the only change occurred in the electrostatic field around it. The electronic part also includes a sum over all charges, even if the latter have not been changed in the MC step.

Alternatively, the value can be approximated by perturbation theory. The difference in the Coulomb operator from the initial and final states corresponds to the perturbation. In first-order, this is given by

$$\Delta(E_{\mathrm{QM}} + E^{\mathrm{C}}_{\mathrm{QM/MM}}) \approx \langle \Psi | \sum_i \sum_\alpha{}' \left(\frac{q_\alpha}{|\mathbf{r}'_\alpha - \mathbf{r}_i|} - \frac{q_\alpha}{|\mathbf{r}_\alpha - \mathbf{r}_i|} \right) | \Psi \rangle + \sum_A \sum_\alpha{}' \left(\frac{q_\alpha Z_A}{|\mathbf{r}'_\alpha - \mathbf{r}_A|} - \frac{q_\alpha Z_A}{|\mathbf{r}_\alpha - \mathbf{r}_A|} \right). \tag{3}$$

The energy change is now calculated by two rather simple sums. The electronic part corresponds to trivial nuclear interaction integrals on the basis of the original wave function. This will, of course, only hold as long as the perturbation is small. Extension to second-order perturbation theory would include density relaxation effects (such as in the approach suggested by Gao and co-workers[25]). Although this is straightforward and could contribute to a better coupling to the environment, it would lead to a break-down of the 2-body interaction potential.

We have opted for a different approach. Technically, the use of Eq. (3) would imply that the QM wave function/density only needs to be recomputed if the solute moves. However, one can also perform updates in the QM density in regular intervals, thereby adapting the latter to the changes in the solvent. This will keep the effect of the perturbation small and the approximation more reliable. We will discuss the effect of such updates later in the text.

With the use of first-order perturbation theory, two major goals are achieved. First of all, the computation of the QM/MM electrostatic interactions is extremely facilitated. Second, and perhaps the most important fact, one obtains an energy expression for use in MC simulations which is strictly based on 2-body interactions. In between density updates, a large number of solvent movements can be carried out using Eq. (2) for the electrostatic component, leading to an effective sampling of the environment.

Our implementation of the PMC QM/MM method works in two main cycles.

(a) *QM update*—the electronic density of the QM region is constructed (in this work we have applied DFT so that this step consists of solving the corresponding SCF cycles).

(b) *PMC cycle*—K PMC steps are taken in the MM system, while keeping the QM region static. The density from the previous QM update is used. Each step consists in selecting, translating, and rotating a random MM molecule (Fig. 1). After this perturbation, the changes in the van der Waals and Coulomb energy of the system must be computed and checked for acceptance.

The Coulomb QM/MM procedure, whereby the charge-electron interaction integrals are computed, stands as the bottleneck of each *PMC cycle* step. The interested reader should refer to Ref. 24 for details on the GPU implementation and how the two cycles can be overlapped for maximal computational efficiency.

In order to compute periodic systems, special care has to be taken about electrostatics since the latter are long-ranged and their contribution non-convergent. The most standard approach to the problem is the use of Ewald summations or methods thereof derived. We opted for a different approach. QM periodic calculations are usually carried out in small simulation boxes, given the inherent computational cost and unfavourable scaling with system size. In such cases, an Ewald sum stands as the most reasonable option. However, since the environment is described at the MM level, we can increase its size with relative ease and routinely compute large simulation boxes, much larger than plane wave calculations or other periodic QM alternatives. With large box lengths, the use of shifted potentials becomes viable.[26] We have opted for the functional form

$$V_{\mathrm{shift}} = \begin{cases} \frac{1}{r} - \frac{1}{r_{\mathrm{c}}} + \frac{1}{r_{\mathrm{c}}^2}(r - r_{\mathrm{c}}) & r < r_{\mathrm{c}} \\ 0 & r \geq r_{\mathrm{c}} \end{cases}. \tag{4}$$

It has been shown for classical simulations that the energetics and dynamics are reproduced remarkably well by a shifted force potential. Energy difference, velocity, and torque vectors have been compared to results from the Ewald summation and they are nearly identical. Furthermore, velocity autocorrelation functions and powerspectra have been compared to evaluate the short- and long-time dynamics which again compare well to the reference.[26]

For each {*atom, grid point*} pair, the corresponding energy variation term is computed, according to their distance in space. This variation is in respect to the previous set of coordinates of the changed molecule. The usage of a cutoff distance results in four possible space regions and four slightly different energy expressions. However, the computation of the $\Delta E^{\mathrm{C}}_{\mathrm{MM}}$ and $\Delta E^{\mathrm{vdW}}_{\mathrm{MM}}$ terms has similar algorithm structures and this leads to no significant penalty in the performance.

A. Density update

The density updates can be carried out with varying frequency. The theoretical limits are well defined with the exact QM/MM simulation on the one side and the frozen density approximation on the other. However the result of the frozen density approximation depends strongly on the actual solvent configuration in which the density is generated. Free energy

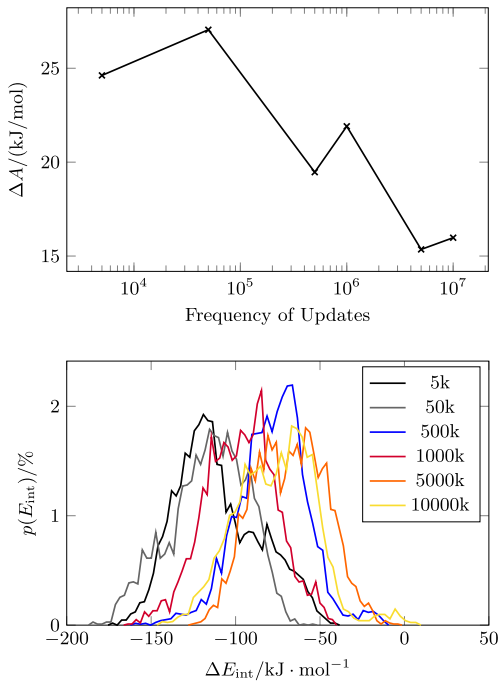

FIG. 2. Free solvation energy simulations with PMC with increasing frequency of density updates for one QM water in the TIP3P solvent. Top: First λ step. Bottom: Distributions of interaction energies between QM and environment.

perturbation (FEP) calculations have been carried out to compute the absolute solvation free energy of water in water. Water as a strongly polar medium is expected to show a strong dependence on the updates and is well-suited as a hard benchmark system. The results in Fig. 2 show the first step of the decoupling of the electrostatic interaction between the QM subsystem and the MM environment. Simulations have been carried out with increasing frequency of density updates. A single MC chain with 40 M steps has been analyzed.

The simulations indicate that the free energies of simulations are very stable with regard to the number of updates. The result changes by only about 2 kJ/mol when the number of updates is increased up to 50 k steps. Decreasing the updates even further to 5 M steps, only 8 densities are generated for the whole simulation. Here a much larger deviation becomes apparent. This is a prototypical example for the dependence on the updates. However, the sign of the deviation can be easily reversed and it depends in the case of very few updates strongly on the configurations which are used for these updates.

The influence on the set of configurations that is generated during the simulations can be very well monitored with the distribution of interaction energies between the QM water and the solvent. As shown in Fig. 2, the shift in these distributions follows the trend observed in the free solvation energies. It becomes evident that not only the energetics are influenced but also that a different part of the configurational space is sampled with less updates. Based on these results, we opt for an update frequency of 20 k steps which strikes a good balance between computational costs and accuracy. The choice has been made based on the study of several simulations. We provide a few more examples in the supplementary material.

B. Integration grid

The accuracy of the computed electrostatic interaction depends not only on the QM update frequency but also on the underlying grid used for the numerical integration. The grids for the description of the electronic charge density were constructed by following the scheme of Mura and Knowles[27] (α = 1 and m = 3) or Becke[28] (α = 1) for the radial distribution and the scheme of Lebedev[29] ($l_{\max}$ = 53) for the angular distribution.

The dependence on the radial distribution of the grid has been investigated on 85 snapshots of a simulation of a capped arginine cation in TIP3P water. The exact electrostatic interaction has been computed with Molpro by neglecting periodicity and compared with the results from the grids. The root-mean square deviations (RMSDs) between grid and exact results are shown in Fig. 3. Both grids converge to the exact result with increasing target accuracy and differences are only visible for a low accuracy. With a target accuracy of 10^{-7} or smaller, the errors are below 0.6 kJ/mol for both grids.

In order to evaluate the impact of the grid target accuracy on the stability of the simulation, PMC simulations starting from the same structure and with the same seeds have been carried out. In Fig. 4, the relative potential energy is plotted for simulations with varying grid sizes, using a simulation with

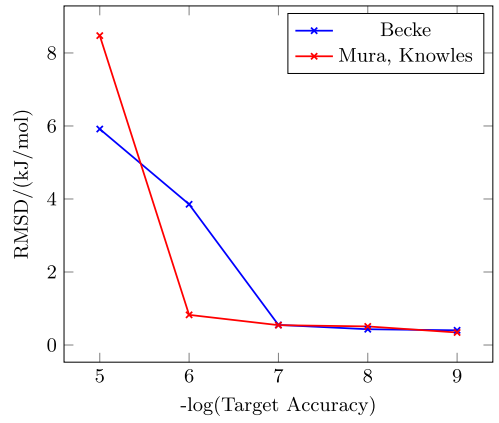

FIG. 3. RMSD of the electrostatic interaction for different grids with the exact results as a reference for snapshots of a PMC simulation of a capped arginine cation in TIP3P water.

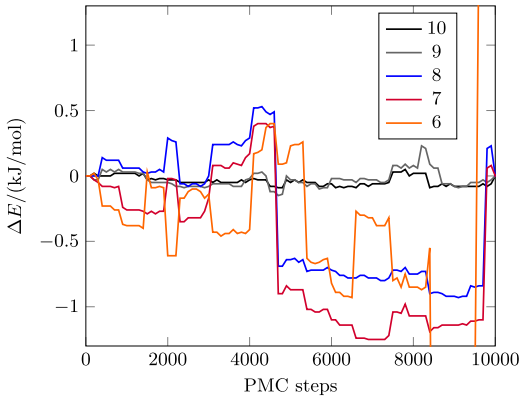

FIG. 4. Comparison of relative potential energies of PMC simulations of the same trajectory with different grid sizes. – log(target accuracy) is given in the legend with the reference being 11.

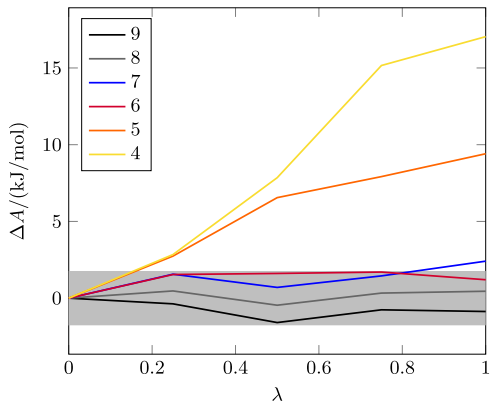

FIG. 5. Decoupling of the electrostatic interaction of a free energy perturbation calculation for ethanol in water with PMC with different grid sizes. – log(target accuracy) is given in the legend and the energies are relative to 11. The shaded area denotes 5% of the free energy (≈1.8 kJ/mol).

a 10^{-11} E_h grid as reference. One can see that with an accuracy of 10^{-10} and 10^{-9} E_h, the error is well below 0.5 kJ/mol. For 10^{-8} and 10^{-7} E_h, the error increases up to about 1.2 kJ/mol.

It is important to note that the structures are exactly the same during this window. An exception is the simulation with an accuracy of 10^{-5} E_h. The difference in the energies is large enough that at about step 8200, the Metropolis MC acceptance criteria produce a different geometry and the Markov chains diverge from each other. At this point, the simulation cannot be compared directly to the reference. Due to the way the Markov chains are constructed, the error does not accumulate over the course of the simulation.

After this detailed comparison of single energy terms and Monte Carlo steps, the overall effect of the grid on a free energy perturbation simulation has been evaluated. The free energy of solvation has been computed for a single ethanol molecule in water. The results of the first half of this simulation—the electrostatic decoupling—are shown in Fig. 5. The target accuracy for the grid has been varied between 10^{-4} and 10^{-11} E_h. It can be seen that the difference between the more accurate grids is lower than 5% of the free energy or about 1.8 kJ/mol. Most importantly, the error does not accumulate with the FEP steps and is well within the limits of the statistical precision of these simulations. This explains also the rather arbitrary ordering of the results. Due to the non-systematic nature of the error, the overall effect on the simulations is rather low even for small grids with a target accuracy of up to 10^{-6} E_h. If the grid size is even further reduced, a systematic overestimation of the free energy can be observed and the error is an order of magnitude larger and accumulates with the lambda steps.

III. COMPUTATIONAL DETAILS

All QM calculations in the PMC simulations described in this manuscript have been carried out with a development version of Molpro.[30] Unless otherwise noted, B3LYP/def2-TZVP[31] including a D3 dispersion correction[32,33] with Becke-Johnson type damping[34] has been used. A level shift of −0.3 E_h has been applied to improve the convergence of the SCF QM calculations. The integration grid for the perturbative steps has been constructed according to Mura and Knowles[27] for the radial grid and according to Lebedev for the angular grid[28] with an increased target quadrature accuracy in Molpro of 10^{-7} E_h for the computation of the density and the default settings for the computation of the energy. Updates of the density have been carried out every 20 k steps.

The different solvent molecules have been described by the OPLS-AA force field, always using a rigid internal geometry. Periodic boundary conditions and cutoffs for the van der Waals and electrostatic interactions of 10 Å and 12 Å, respectively, have been used for all simulations. A temperature of 298 K has been used for simulations or free energy corrections. The step size of the Monte Carlo translational steps has been adjusted in order to achieve an acceptance ratio of about 20% and the rotation steps fixed to 10°.

The tests for different grids featured in Sec. II B have been carried out with density-fitting[35] approximations and the PBE[36] functional.

Free energy differences with the PMC approach have been computed by the use of free energy perturbation theory (FEP) protocols. Simulations have been carried out in forward and reverse directions. Uncorrelated frames of these simulations have been analysed with the Bennett acceptance ratio (BAR) method.[37] Autocorrelation functions as well as BAR were computed through the use of the pymbar program.[38,39]

IV. RESULTS AND DISCUSSION

Benchmarking computational methods for systems in solutions can be an intricate task. Aside from solvation energies, there are little experimental data which can be compared to theory in a straightforward fashion. Concentration effects, diffusion, and the inherent difficulty of measuring data in solution all lead to an uncertainty whether deviations are due to the model being used or inherent to the experiment. With this in mind, we considered three main questions to be tackled in our test applications:

(a) solvent structure, particularly the structure of the first solvation shells around the QM solute.
(b) Thermodynamics of solvation, which are considered through the calculation of solvation free energies.
(c) Solvent effects on reactivity, namely, the stabilization of transition states and/or products.

A. Methyl chloride solvation shell

Solvent effects can be classified according to the dominant physical interactions at play. The first would be the electrostatic interaction between the solvent and solute. Another factor in play is the additional sterical hindrance caused by the solvent[40] or dispersion effects which can become quite significant in the condensed phase. The change of the potential energy of the solute can be roughly distinguished in three categories. The direct effect shifts the energies of stationary points, the geometric effect changes the positions of the stationary points itself, and the vibrational effect changes the curvature of the potential energy surface, modifying the vibrational levels and consequently also the free energy.[41]

Nucleophilic substitution reactions (S_N2) of methyl halides

$$X^- + RY \rightarrow XR + Y^-$$

have been widely studied over the years and the solvent influence on this class of reactions has been well established.[40–44] For example, the potential of reactions with R = CH_3 and X, Y = Cl changes from a double well potential in gas-phase to a unimodal potential in an aqueous environment. This causes transfer rates to be lowered up to 20 times.

Directional interactions, e.g., hydrogen bonds, are of high importance since they may stabilize specific phase space points along the reaction coordinate.[44] The PMC QM/MM approach, by allowing the explicit simulation of the solvent structure, could in principle describe such effects. However, for this to happen, the molecular interactions have to be properly described. Since the solute-solvent interactions are described through classical Lennard-Jones potentials and an electrostatic interaction term which is only correct up to first-order, the accuracy of the method should be carefully assessed.

We have studied the solvation shell structure of methylchloride (MeCl), a commonly used model for this type of reactions. It is known that simple force fields for water have issues in the description of local hydrogen bonding structures. It has been argued that in the context of QM/MM, many of the hydrogen bond properties can be reproduced.[45] We have carried out PMC calculations of MeCl in aqueous solution and analysed the solvent structure, making use of geometry criteria.

A PMC QM/MM simulation of 80 M steps has been carried out with density updates every 20 k steps. Snapshots were saved every 10 k steps and used for further analysis. For comparison, classical MM MC simulations have been carried out with the same number of steps, whereby also the solute is described with the OPLS-AA force field.

The distance and angle are defined as depicted in Fig. 6 together with the corresponding angular radial distribution functions. In the case of PMC QM/MM, a sharp peak is visible at distances of 2.0-2.5 Å and below 35°. This peak accounts for the interaction between the chloride and its first solvation shell. Angles smaller than 30° are indicative of hydrogen bonds.[44] In contrast, the wide range of angles at longer distances which can be observed in the MM MC results is typical for non-directional interactions. The PMC results are in qualitative agreement with Car-Parrinello MD simulations[44] on a similar system $[Cl \cdots CH_3 \cdots Br]^-$.

B. Solvation free energies

Solvation free energies are not only of importance for chemistry but also for biology and pharmacy. Relevant processes that are influenced are protein folding, protein-ligand binding, or the transport of drugs across membranes.[46] Since many experimental results are available for small molecules in a wide range of solvents, the computation of solvation free energies poses an important benchmark for any new method or force field.[47] It should be noted, however, that this is far from being the type of application one would be interested in the use of PMC QM/MM. Classical MM and continuum models can, with adequate parameterization, perform quite well in such applications.

The internal geometries of all solutes have been optimized in gas phase and with COSMO with the following dielectric constant values: ϵ(Toluene) = 2.379, ϵ(Chloroform) = 4.806, ϵ(Acetonitrile) = 35.88, ϵ(Water) = 80.0. Solvation free energies are straightforward to compute. The interaction between the QM subsystem and its surrounding is stepwise decoupled by scaling the point charges or van der Waals parameters. The electrostatic interaction has been turned off in four equidistant steps. In cases of large differences between the forward and reverse simulation, the number of steps has been doubled. This only occurred for the

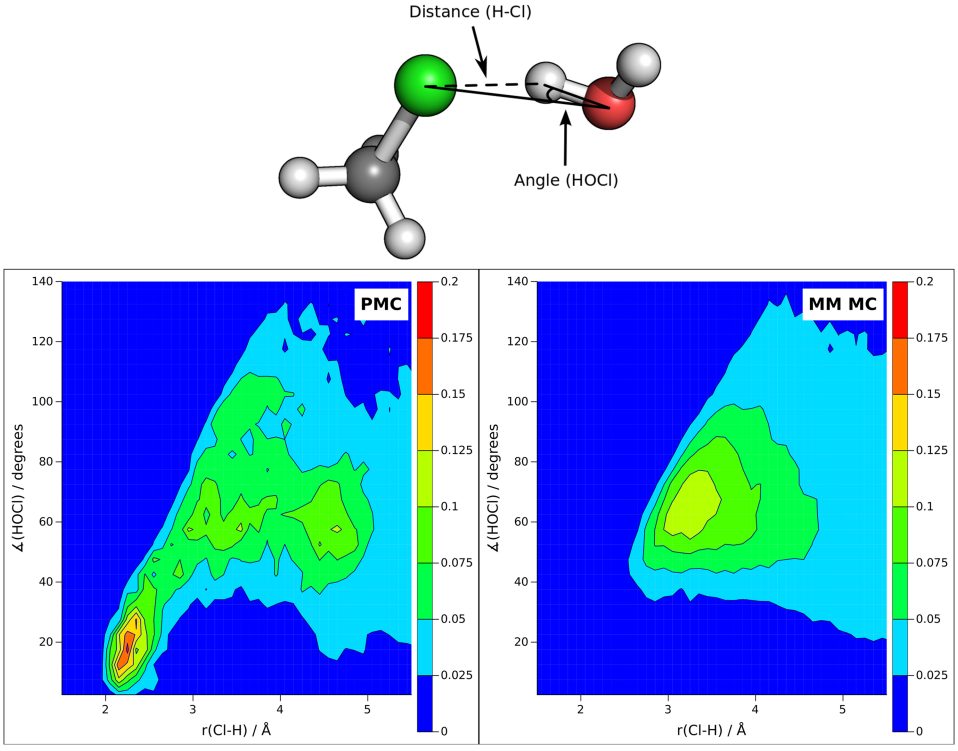

FIG. 6. Top: Definitions of distance and angle. Bottom: Radial angular distribution function of $ClCH_3 \cdots F^-$ in TIP3P water simulated with PMC (B3LYP/def2-TZVP) and MM MC (OPLS-AA).

solvent water with the solutes water, toluene and ethane-1,2-diol.

The decoupling of the van der Waals interaction requires a soft-core potential[48] which explicitly depends on the alchemical variable λ and thereby avoids singularities with the numerical integration of FEP at the endpoints. The van der Waals interaction is then defined as

$$E_{\mathrm{vdW}} = 4\epsilon\lambda^n \left[\left(\alpha\,(1-\lambda)^m + \left(\frac{r}{\sigma}\right)^6 \right)^{-2} - \left(\alpha\,(1-\lambda)^m + \left(\frac{r}{\sigma}\right)^6 \right)^{-1} \right] \tag{5}$$

with $m = n = 1$, $\alpha = 0.5$, and ϵ and σ defining the van der Waals potential.

The λ schedule for the decoupling of the van der Waals interactions has been chosen according to Sherman *et al.*[46] in order to ensure accuracy and stability of the simulations. PMC simulations of 10 M steps for every λ step with 4 M intermediate steps have been carried out.

The solute geometry is kept fixed during the desolvation; therefore, a contribution for the geometry relaxation has to be added. This has been computed as the energy difference between the solvent geometry in vacuum and the optimized vacuum geometry. Corrections for the free energy contributions due to changes of the vibrations of the solute have been estimated by computing the thermal corrections with COSMO and in vacuum.

29 different combinations of solutes and solvents have been selected and the results are represented in Fig. 7 in comparison with experimental results.[49] The standard deviation as derived by Bennett[37] [see Eq. (10a), with $n_1\langle f\rangle_1^2$ in the second denominator, that is a typing error in the original paper] is visualized by the error bars and given in Table I. The standard deviation depends on the number of MC steps and the overlap of the configurational spaces. The more dissimilar the two states, the more the steps required to keep a constant standard deviation. This estimates the statistical precision of the results and not underlying errors in the potential.

In general, a reasonable agreement is observed, meaning that the model captures the majority of interactions at play. In a recent study[50] with the solvents water and chloroform, it has been noted as well that QM/MM does not always improve upon the MM results and that the accuracy may be, for this particular application, comparable. The advantage over other approaches is that very few parameters are required for the setup. Force fields for the solvent description are very well established and readily available. The required van der Waals parameters for the solute do not influence the results significantly.

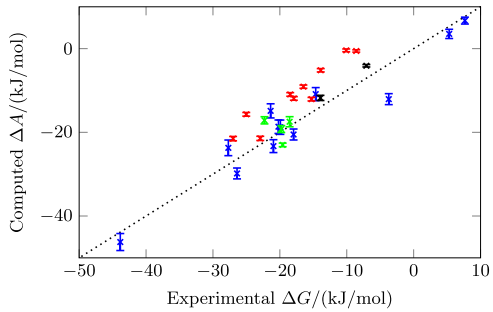

FIG. 7. Solvation free energies computed with PMC in comparison with experimental results. The solutes and solvents are listed in Table I.

TABLE I. All combinations of solute and solvent that have been used, free energies of solvation (Comp.), estimated error bar (Prec.) and experimental results (Expt.).[49] All energies are given in kJ/mol.

Solute	Solvent	Comp.	Prec.	Expt.
Water	Water	−29.8	1.3	−26.4
Ammonia	Water	−20.5	1.3	−18.0
Ethane	Water	6.7	0.8	7.7
Ethene	Water	3.5	1.1	5.3
Methanol	Water	−14.9	1.7	−21.4
Ethanol	Water	−23.3	1.5	−21.0
Ethane-1,2-diol	Water	−64.1	1.7	−38.9
1-Propanol	Water	−18.8	1.7	−19.9
2-Propanol	Water	−18.7	1.6	−20.2
Ethanal	Water	−10.9	1.6	−14.6
Toluene	Water	−12.1	1.3	−3.7
Phenol	Water	−23.8	1.9	−27.7
4-hydroxybenzaldehyde	Water	−46.2	2.0	−43.9
Ethanol	Toluene	−11.8	0.6	−13.9
Water	Toluene	−4.1	0.3	−7.1
Ethanol	Acetonitrile	−17.5	1.2	−18.5
Butanone	Acetonitrile	−19.2	0.8	−19.8
1,4-Dioxane	Acetonitrile	−17.1	0.9	−22.3
Toluene	Acetonitrile	−23.0	0.4	−19.6
Water	Chloroform	−0.6	0.3	−8.6
Ammonia	Chloroform	−0.4	0.3	−10.1
Methanol	Chloroform	−5.2	0.4	−13.9
Ethanol	Chloroform	−9.1	0.4	−16.5
Ethane-1,2-diol	Chloroform	−15.7	0.4	−25.0
1-Propanol	Chloroform	−11.0	0.4	−18.5
2-Propanol	Chloroform	−11.9	0.4	−17.9
Ethanal	Chloroform	−12.1	0.4	−15.3
Toluene	Chloroform	−21.5	0.5	−22.9
Pyridine	Chloroform	−21.5	0.5	−27.0

Surprisingly, some of the largest deviations are found for the chloroform case. A systematic underestimation of the solvation free energies of about 11 kJ/mol in average can be observed. In order to investigate this effect, the partial charges have been adjusted to reproduce the estimated dipole moment in liquid phase. The latter has been computed at the CCSD level using a cc-pVTZ basis set and including COSMO (ϵ = 4.806) corrections consistent with the HF solution (PTE scheme). Simulations with this increased dipole moment showed (Fig. 8) that the energies depend systematically on the dipole moment of the MM model. The average underestimation is reduced by about 1.3 kJ/mol. While the free solvation energies can be influenced strongly, the pure solvent radial distribution functions are very stable with regard to changes of the dipole moment for a given volume and temperature (see the supplementary material).

C. Torsional potential of hydrogen peroxide

In this section, we assess the PMC QM/MM approach in the description of reaction paths, using the torsional potential

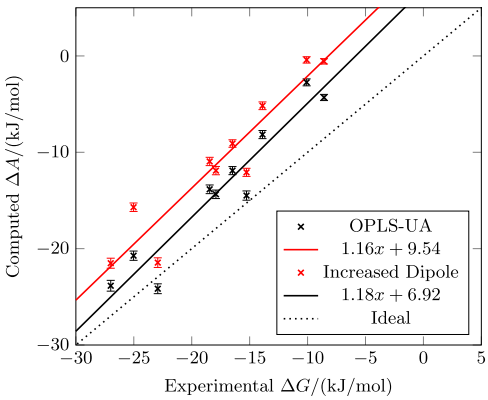

FIG. 8. Solvation free energies computed with PMC in chloroform and chloroform with an increased dipole moment.

of hydrogen peroxide as an example. In order to obtain converged results rather small FEP, steps in the torsional angle have to be used. This is more efficient than using longer simulations for larger steps because the phase space overlap is increasing with decreasing stepsize. However, the simulations are much more demanding than computations of solvation free energies. The hydrogen peroxide potential has been computed in 2.5° steps for 20 M PMC steps with density updates every 1000 steps. 2 M intermediate PMC steps have been carried out in order to reach equilibrium for the adjusted geometries. In this case, we opted for a larger number of updates (1000 vs 20 000) to improve the stability of the numerical results. The change did not lead to any computational bottleneck since the QM calculations are performed overlapping with the MM and the QM system was rather small in size (Fig. 9).

A comparison of gas phase results and in solution (Fig. 9) shows that a large solvent effect is present. The stationary points are clearly influenced. The cisoid transition state is strongly stabilized by about 10 kJ/mol, independent of the method of choice. The COSMO results show inversely a destabilization of the transoid transition state by about 2 kJ/mol, while the PMC simulations predict a stabilization of this transition state by the same amount. This difference can be explained by specific interactions—hydrogen peroxide is a hydrogen bond donor as well as acceptor—which can be described by COSMO only approximately at best. These findings are

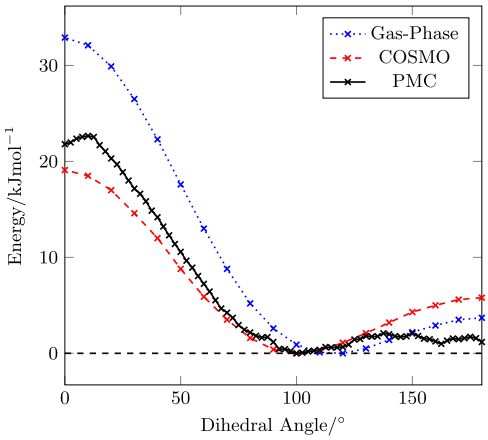

FIG. 9. The torsional potential of hydrogen peroxide computed in gas phase, with COSMO (ϵ = 80) and in TIP3P water with PMC.

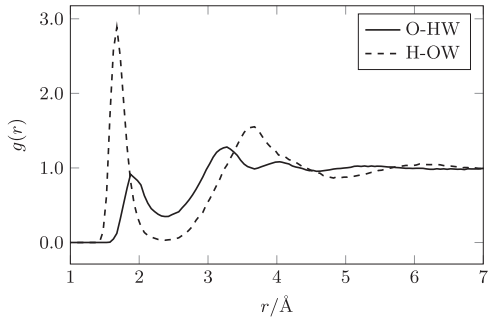

FIG. 10. Radial distribution function $g(r)$ of donating (O–HW) and accepting (H–OW) hydrogen bonds of hydrogen peroxide.

in agreement with QM/MM replica exchange MD (REMD) studies,[51] which predict a slightly larger stabilization of 15 kJ/mol of the cisoid and a stabilization of about 2 kJ/mol of the transoid transition state. The position of the minimum on the other hand agrees very well for both methods and is located at about 100°. This is in qualitative agreement with the QM/MM REMD simulations of Choi and co-workers who predict a minimum slightly above 90°. In gas phase, the minimum is at about 120°. This makes the test system of particular interest, given that it is not only the energy differences between the stationary points that are changing but also their geometry.

Hydrogen peroxide is known to be a better hydrogen bond donor than acceptor. In order to investigate, if the PMC simulations reproduce this important property, not only qualitatively but also quantitatively, the radial distribution functions at the minimum have been analyzed. It is expected that the donating hydrogen bond length is shorter and that the first peak is more prominent compared to the accepting hydrogen bond. The results are shown in Fig. 10 confirming the above mentioned trends. The positions of the first and second solvent peaks are also compared with other theoretical studies in Table II. The results closely match the results of a QM/MM MD study by Martins-Costa and Ruiz-López with a similar combination of methods.[52] The hydrogen bond lengths are slightly longer than Born-Oppenheimer MD (BOMD) simulations[53] by up to 4%. This is an excellent agreement which shows that donating and accepting bonds—which pose a very different requirement to QM/MM approaches—can be equally well described. Recent classical simulations[54] show a much larger deviation but reproduce qualitatively the first two peaks.

TABLE II. Comparison of the peak positions of the RDFs shown in Fig. 10 with results from Cabral: BOMD (B3LYP-D3), Ruiz-Lopéz: QM/MM MD (B3LYP/6-31G*, TIP3P) and Coutinho: MM MC.

		PMC	Cabral[53]	Ruiz-Lopéz[52]	Coutinho[54]
O–HW	1st	1.89	1.91	1.85	2.08
	2nd	3.28	3.24	3.26	3.42
	3rd	4.03	4.18	4.02	...
H–OW	1st	1.67	1.74	1.64	1.81
	2nd	3.65	3.65	3.61	3.81

V. CONCLUSIONS

In this work, we present an efficient implementation of the perturbative QM/MM Metropolis Monte Carlo scheme of Truong and Stefanovitch for hybrid architectures, with the extension to periodic systems. Through the concurrent use of CPU and GPU, it is possible to perform millions of QM/MM MC steps in a day using a single workstation, enabling QM/MM FEP calculations with demanding DFT electronic structure methods. We have analysed in detail the impact of the numerical approximations involved, namely, the QM update frequency and the DFT grid for QM/MM electrostatic interactions. Our results show that even for strongly polar systems, the wave function/density only needs to be updated every 10-20 k PMC steps, and moderately sized integration grids suffice to keep numerical stability and accuracy.

Several applications have been presented, from solvation energies to the solvent effect on activated processes. Overall, we observe that the accuracy of the method is competitive with commonly used continuum models, while offering some specific advantages. These include information about the solvent structure, the lack of parameterization (beyond the definition of the molecular force field for the environment), and the possibility of describing heterogeneous environments. The latter was not a focus of this work. In the future, we intend to explore the use of PMC in the description of solvent mixtures and supramolecular host-guest systems.

SUPPLEMENTARY MATERIAL

See supplementary material for additional data from free solvation energy simulations with different update frequencies as well as the radial distribution functions of pure chloroform with increased dipole moment.

ACKNOWLEDGMENTS

This work was partially supported by Portuguese national funds through Funda cão para a Ciência e a Tecnologia (FCT) under projects Threads (Ref. No. PTDC/EEA-ELC/117329/2010), P2HCS (Ref. No. PTDC/EEI-ELC/3152/2012) and Project No. PEst-OE/EEI/LA0021/2013. Financial support from the Deutsche Forschungsgemeinschaft through Grant No. SFB1073 is gratefully acknowledged.

[1] E. Harder, W. Damm, J. Maple, C. Wu, M. Reboul, J. Y. Xiang, L. Wang, D. Lupyan, M. K. Dahlgren, J. L. Knight, J. W. Kaus, D. S. Cerutti, G. Krilov, W. L. Jorgensen, R. Abel, and R. A. Friesner, J. Chem. Theory Comput. **12**, 281 (2016).
[2] S. Belsare, A. Esser, D. Marx, and T. Head-Gordon, Biophys. J. **112**, 497a (2017).
[3] S. Grimme, J. Chem. Theory Comput. **10**, 4497 (2014).
[4] G. Jindal and A. Warshel, J. Phys. Chem. B **120**, 9913 (2016).
[5] M. W. van der Kamp and A. J. Mulholland, Biochemistry **52**, 2708 (2013).
[6] E. Boulanger and W. Thiel, J. Chem. Theory Comput. **10**, 1795 (2014).
[7] J. C. Richley, J. N. Harvey, and M. N. R. Ashfold, J. Phys. Chem. C **116**, 18300 (2012).
[8] D. Golze, M. Iannuzzi, M.-T. Nguyen, D. Passerone, and J. Hutter, J. Chem. Theory Comput. **9**, 5086 (2013).
[9] D. Golze, J. Hutter, and M. Iannuzzi, Phys. Chem. Chem. Phys. **17**, 14307 (2015).
[10] O. Andreussi, I. G. Prandi, M. Campetella, G. Prampolini, and B. Mennucci, J. Chem. Theory Comput. **13**, 4636 (2017).
[11] A. Klamt and G. Schüürmann, J. Chem. Soc., Perkin Trans. 2 **1993**, 799.
[12] S. Miertuš, E. Scrocco, and J. Tomasi, Chem. Phys. **55**, 117 (1981).
[13] A. V. Marenich, C. J. Cramer, and D. G. Truhlar, J. Phys. Chem. B **113**, 6378 (2009).
[14] A. Klamt, J. Phys. Chem. **99**, 2224 (1995).
[15] D. Beglov and B. Roux, J. Phys. Chem. B **101**, 7821 (1997).
[16] A. Kovalenko and F. Hirata, Chem. Phys. Lett. **290**, 237 (1998).
[17] P. H. Fries and G. N. Patey, J. Chem. Phys. **82**, 429 (1985).
[18] F. Hirata and P. J. Rossky, Chem. Phys. Lett. **83**, 329 (1981).
[19] A. Kovalenko and F. Hirata, J. Chem. Phys. **110**, 10095 (1999).
[20] J. Heil and S. M. Kast, J. Chem. Phys. **142**, 114107 (2015).
[21] A. Kovalenko and T. N. Truong, J. Chem. Phys. **113**, 7458 (2000).
[22] T. Schlick, *Innovations in Biomolecular Modeling and Simulations* (Royal Society of Chemistry, 2012).
[23] T. N. Truong and E. V. Stefanovich, Chem. Phys. Lett. **256**, 348 (1996).
[24] S. Miranda, J. Feldt, F. Pratas, R. A. Mata, N. Roma, and P. Tomás, Int. J. High Perform. Comput. Appl. **31**, 499 (2017).
[25] E. Cubero, F. J. Luque, M. Orozco, and J. Gao, J. Phys. Chem. B **107**, 1664 (2003).
[26] C. J. Fennell and J. D. Gezelter, J. Chem. Phys. **124**, 234104 (2006).
[27] M. E. Mura and P. J. Knowles, J. Chem. Phys. **104**, 9848 (1996).
[28] A. D. Becke, J. Chem. Phys. **88**, 2547 (1988).
[29] V. Lebedev, USSR Comput. Math. Math. Phys. **15**, 251 (1975).
[30] H.-J. Werner, P. J. Knowles, G. Knizia, F. R. Manby, M. Schütz *et al.*, MOLPRO, version 2012.1, a package of *ab initio* programs, 2012, see www.molpro.net.
[31] F. Weigend and R. Ahlrichs, Phys. Chem. Chem. Phys. **7**, 3297 (2005).
[32] S. Grimme, J. Antony, S. Ehrlich, and H. Krieg, J. Chem. Phys. **132**, 154104 (2010).
[33] S. Grimme, S. Ehrlich, and L. Goerigk, J. Comput. Chem. **32**, 1456 (2011).
[34] E. R. Johnson and A. D. Becke, J. Chem. Phys. **123**, 024101 (2005).
[35] R. Polly, H.-J. Werner, F. R. Manby, and P. J. Knowles, Mol. Phys. **102**, 2311 (2004).
[36] J. P. Perdew, K. Burke, and M. Ernzerhof, Phys. Rev. Lett. **77**, 3865 (1996).
[37] C. H. Bennett, J. Comput. Phys. **22**, 245 (1976).
[38] J. D. Chodera, W. C. Swope, J. W. Pitera, C. Seok, and K. A. Dill, J. Chem. Theory Comput. **3**, 26 (2006).
[39] M. R. Shirts and J. D. Chodera, J. Chem. Phys. **129**, 124105 (2008).
[40] B. Ensing, E. J. Meijer, P. E. Blöchl, and E. J. Baerends, J. Phys. Chem. A **105**, 3300 (2001).
[41] M. Cossi, C. Adamo, and V. Barone, Chem. Phys. Lett. **297**, 1 (1998).
[42] C. K. Regan, S. L. Craig, and J. I. Brauman, Science **295**, 2245 (2002).
[43] T. N. Truong and E. V. Stefanovich, J. Phys. Chem. **99**, 14700 (1995).
[44] M. Pagliai, S. Raugei, G. Cardini, and V. Schettino, J. Mol. Struct.: THEOCHEM **630**, 141 (2003).
[45] K. Senthilkumar, J. I. Mujika, K. E. Ranaghan, F. R. Manby, A. J. Mulholland, and J. N. Harvey, J. R. Soc. Interface **5**, 207 (2008).
[46] D. Shivakumar, J. Williams, Y. Wu, W. Damm, J. Shelley, and W. Sherman, J. Chem. Theory Comput. **6**, 1509 (2010).
[47] P. F. B. Gonçalves and H. Stassen, Pure Appl. Chem. **76**, 231 (2004).
[48] J. W. Pitera and W. F. van Gunsteren, Mol. Simul. **28**, 45 (2002).
[49] G. D. Hawkins, C. J. Cramer, and D. G. Truhlar, J. Phys. Chem. B **102**, 3257 (1998).
[50] M. Wang, P. Li, X. Jia, W. Liu, Y. Shao, W. Hu, J. Zheng, B. R. Brooks, and Y. Mei, J. Chem. Inf. Model. **57**, 2476 (2017).
[51] D. G. Fedorov, Y. Sugita, and C. H. Choi, J. Phys. Chem. B **117**, 7996 (2013).
[52] M. T. C. Martins-Costa and M. F. Ruiz-López, Chem. Phys. **332**, 341 (2007).
[53] B. J. C. Cabral, J. Chem. Phys. **146**, 234502 (2017).
[54] M. C. Caputo, P. F. Provasi, L. Benitez, H. C. Georg, S. Canuto, and K. Coutinho, J. Phys. Chem. A **118**, 6239 (2014).